

Numerical Modeling of Polymer Electrolyte Fuel Cell Catalyst Layer with Different Carbon Supports

I.E. Baranov, I.I. Nikolaev, A.S. Pushkarev, I.V. Pushkareva, A.A. Kalinnikov, V.N. Fateev*

NRC “Kurchatov Institute”, 123182, Russia, Moscow, Kurchatov sq., 1

*E-mail: pushkarev_as@outlook.com, fateev_vn@nrcki.ru

Received: 12 December 2017 / Accepted: 12 July 2018 / Published: 5 August 2018

The Monte Carlo simulation method is used to carry out numerical modelling of the polymer electrolyte membrane fuel cell (PEMFC) catalyst layer with a random catalyst particles distribution in a polymer matrix. The approaches of mass transport and electrochemical kinetics are applied for estimation of potential distribution and current generation in the catalyst layer. It is shown that large particles of the catalyst support (agglomerates of nanofibers) provide percolation for electron transport at a lower concentration in comparison with compact catalyst support particles (i.e. Vulcan XC-72R). Mixtures of such supports also have a lower percolation threshold. It gives the possibility to increase polymer concentration, stabilise water balance and decrease ohmic losses for ion transport in the catalyst layer. The numerical estimations demonstrate the possibility of precious metal loading reduction up to 30% and the increase of performance (current density) up to 20% just due to addition of carbon nanofibers in the catalyst layers. In the experimental study we reached an increase of PEMFC current density for about 10% when we used the Vulcan XC-72R supported Pt catalyst together with the Pt catalysts on nanofibres

Keywords: Catalyst Layer, Numerical Simulation; Polymer Electrolyte Fuel Cell; Percolation, Pt Based Electrocatalysts, Catalyst Supports.

1. INTRODUCTION

Membrane electrode assembly (MEAs) and catalyst layers are the key components of a polymer electrolyte membrane fuel cell (PEMFC). The catalyst layer structure and composition determine a fuel cell efficiency, precious metal loading and a fuel cell durability. At the present time different types of carbon catalyst carriers are used for the PEMFC including graphene nanoribbons (flakes), carbon nanotubes and nanofibers [1-4]. In some investigations [5-8] an increase of the catalyst layer activity was observed when such materials were added to the layers based on a more traditional

carbon carrier like Vulcan XC-72. So, catalyst carriers play an important role in the PEMFC performance.

Modeling of the PEMFC and especially the modeling of catalyst layers is a rather important problem and investigations in this field were started at the end of the last century by different researchers (e.g. [9-11]). Usually micro-scale [9-10] and macro-scale [11-14] approaches are used to estimate the catalyst layer efficiency at different operating conditions. In some investigations the catalyst layer was represented as a porous matrix consisting of a uniform mixture of Pt, carbon and ionomer (homogeneous model) and the real layer structure was practically ignored [12-13]. The agglomerate model [11-14], where carbon-platinum aggregates are considered, is more efficient from our point of view. Earlier [15-19] theoretical approaches for the catalyst layer modeling based on the Monte Carlo method, the mass transport theory and electrochemical kinetics approaches were developed. In this model the dependence of the catalyst particles activity upon their size and distribution in the catalyst layer together with the catalyst layer structure were considered.

The model described above and the appropriate software [20] are used in this research for the modeling of catalyst layers based on carbon supports (carriers) of different type and their mixtures for the catalyst layer structure and composition optimization.

2. EXPERIMENTAL

2.1 Modeling approach

The Monte Carlo simulation method was used to carry out numerical modeling of catalyst layer with a random catalyst particles distribution in a uniform porous polymer (ionomer) matrix. The approaches of mass transport and electrochemical kinetics were used for the estimation of potential distribution and current generation in the catalyst layer [15-19]. All numerical calculations were done using the self-developed software developed [20]. Three percolation systems (catalyst – electron transport, ionomer – ion transport, pores – reactant/product transport), according to the model, must exist in the catalyst layer. A catalyst particle can be active (takes part in electrochemical process) only if it is electronically connected with other catalyst particles and/or a gas diffusion layer (GDL). Moreover, a catalyst active particle must have a contact with the active “particle” of an ionomer and the activity of such particles depends upon the potential distribution in the catalyst layer and the efficiency of reactant (product) transport. The amount of such active particles was numerically estimated using Monte Carlo simulation.

The initial purpose of the numerical simulation was to estimate such catalyst layer parameters as conductivity and surface area of the conductive particles in the layer depending upon volume fractions of the catalyst and the ionomer. The calculation took into account the catalyst layer size, particle size, particle shape and pore size.

We considered the catalytic layer to be bounded by two planes – the plane between the membrane and the catalyst layer and the plane between the layer and the GDL. A grid system was introduced. The *Y* and *Z* axes are parallel to the planes of this layer. As the layer size along these axes

is much greater than its thickness (the size along the X axis) these layer dimensions can be considered as infinite..

A rectangular volume inside the layer was taken for the modeling. This volume was split into individual cells by a system of mutually perpendicular planes. The cell size was determined by the ratio of the minimum particle size and the layer thickness. Cells were further randomly filled by particles of several types: electrolyte, catalyst and pores, according to the volume fractions of these components in the catalyst layer. The calculation method allows to consider catalyst particles of any shape or size, as well as a mixture of particles of different sizes. Large particles were simulated by filling multiple cells.

There are two types of current flow are in the catalyst layer: an ion current along the connected ionomer particles and the electron current along the connected catalyst particles. Thus, the catalyst layer contains catalyst particles which have an electrical contact with the GDL (active particles which participate in the electrochemical reaction) and those particles which haven't one. This approach may also be used for ionomer particles which provides the ion current. In our calculations we identified 5 types of particles in the catalyst layer:

1. Catalyst particle with the electronic conductivity not connected with the GDL;
2. Catalyst particle with the electronic conductivity connected with the GDL through the other particles of this type. These active particles are involved in the electrochemical reaction;
3. Ionomer "particles" with the ion conductivity not connected with the membrane;
4. Ionomer "particles" with the ion conductivity connected with the membrane through the other particles of this type. These active particles are involved in the electrochemical reaction;
5. Pores;

The quasi-continuous, periodic boundary conditions were maintained in the calculations along the Y and Z axes on the side faces of the modeled volume in order to consider the infinite size of the layer in these directions. The GDL was simulated as the first layer of particles on the X axis filled with electrically conductive particles. The plane of the membrane was modeled by complete filling of the last layer of particles with electrolyte (ionomer) particles.

Simulation was as follows: first, the cell volume was filled with the simulated particles of three types described above: catalyst particles of type 1, ionomer particles of type 3 and pores (type 5). The filling was fulfilled randomly. The ratio between the number of particles of different types was in accordance with the catalyst layer composition (volumetric fractions). Then a particle of type 1 which lies close to a particle of type 2 were replaced with the last one through multiple iterations by the program. The initial particles of type 1 are the particles of the first layer simulating the GDL. A similar procedure was implemented for ionomer particles (particles of type 3 and 4, respectively).

Thus, after the calculation, all active catalyst particles (type 2) electrically connected with the GDL and the active particles of ionomer ionically connected with the membrane (type 4) were found and identified. Next, the distribution of active particles over the layer thickness and the distribution of the active surface area (the interface between the particles of type 2 and 4) over the layer thickness were found. The simulation was conducted on a grid area with mesh size of $100*100*100$ and was repeated 20 times, after which the obtained results were averaged. It was shown that the error in such a case was less than 3%.

It should be noted that for a continuous media the percolation starts when concentration of any component in the mixture is about 33 vol.%. If the layer has a limited thickness (like the catalyst layer) the situation could be quite different. If the size of catalyst particles is comparable to the layer thickness (for example, about 0.33 of the layer thickness), then they have a high chance to be an active since they have a higher probability to have an electrical contact with the GDL than the smaller particles. But their activity also depends on efficiency of their contact with the ionomer and reactants. A uniform Pt particles distribution on the carbon support surface was supposed. It is worth noting that the resistance of the catalyst particle chains and especially the resistance of the ionomer in the catalyst layer can significantly decrease the catalyst layer efficiency. Estimations of changes in potential difference between catalyst and ionomer in the direction perpendicular to the catalyst layer and their influence on the catalyst layer activity (current density) were done according to the approaches (Eq. 1) developed in [21]:

$$\frac{d\varphi_{c,i}}{dx} = \rho_{c,i} \cdot I_{c,i}(x) \quad (1)$$

where: x – the distance across the catalyst layer, $\rho_{c,i}$ – resistivity of the components (catalyst (c) or ionomer (i) particles), $I_{c,i}$ – generated current, depending on x , $\varphi_{c,i}$ – the potential of the catalyst or ionomer particles, depending on x . In the case of diffusion limitations Fick's law was used and a water convective flow was taken into account (for more details see [15-19]). According to the first approach we made a numerical analysis of the catalyst layer containing 2 types of particles (agglomerates of carbon supports with Pt catalyst particles on their surfaces) with the size 0.4 and 4 μm which were simulating catalysts on two different supports: Vulcan XC-72R (Cabot Corp., USA) and nanofibers (Grupo Graphenano, Spain) respectively. The internal structure of such agglomerates wasn't taken into account and the roughness of their external surface was assumed to be equal to 6 according to the TEM data at first approximation. Here and after in all discussions on the numerical calculation results we use the term "particle" for agglomerates discussed above as it was supposed in the model. The term "cluster" means an association of particles (agglomerates discussed above). The catalyst layer thickness was taken as 12 μm according to the TEM data. The porosity for all calculations was adopted of 30 vol.% according to the BET studies data.

2.2 Catalysts preparation and characterization

The magnetron sputtering method in a pulsed mode [22-26] was used for synthesis of Pt based catalysts (40 wt.% of Pt) on Vulcan XC-72R (Cabot Corp., USA), nanofibers (Grupo Graphenano, Spain) and their mixtures.

Specific surface area and porosity of supports were determined by low temperature adsorption of nitrogen using TriStar 3000 (Micromeritics, USA). The surface area was 240 $\text{m}^2 \text{g}^{-1}$ for Vulcan XC-72R and 160 $\text{m}^2 \text{g}^{-1}$ for nanofibers. TEM images of carbon supports and platinum supported catalysts were obtained using Titan 80-300 S/TEM (FEI, USA).

Pt based catalyst electrochemically active surface area (EASA) was determined according to the cyclic voltammetry (CV) measurements in a three-electrode glass cell according to [25] using

Solartron 1285 (Solartron Analytical, USA). A Pt-foil counter-electrode and a saturated Ag/AgCl reference electrode were used. All measurements were carried out in 1 M H₂SO₄ solution at 25°C.

Catalysts EASA were quite similar for all samples: about 45 m² g⁻¹ for Vulcan XC-72R supported catalyst and about 41 m² g⁻¹ for nanofibers supported one. The average value of 43 m² g⁻¹ was used for numerical calculations. All numerical computations were done for the fuel cell cathode using standard electrochemical parameters of Pt catalysts [16,18].

2.3 MEA preparation and characterization

The fuel cell membrane electrode assemblies (MEAs) with 7 cm² surface area were produced by air-spraying of the catalyst ink/isopropanol solution on the Nafion NRE 212 (DuPont, USA) membrane surface and were tested as described earlier [22] at 75 °C with H₂ (pressure 1 bar, 100% relative humidity) and air (at atmospheric pressure) at anode and cathode, respectively.

3. RESULTS AND DISCUSSION

The TEM images of Vulcan XC-72R and nanofibers supported catalysts are shown in Fig. 1 and Fig. 2. For both catalyst supports a large amount of support particles agglomerates are existed in the catalyst layer (Fig. 1 A, Fig. 2 A) but in the case of nanofibers their size is significantly larger (about 4 μm as opposed to 0.4 μm for Vulcan XC-72R). Pt particles size is about 6-8 nm for Vulcan XC-72R supported catalyst (Fig. 1 B) and about 7-10 nm for the nanofibers supported one (Fig. 2 B).

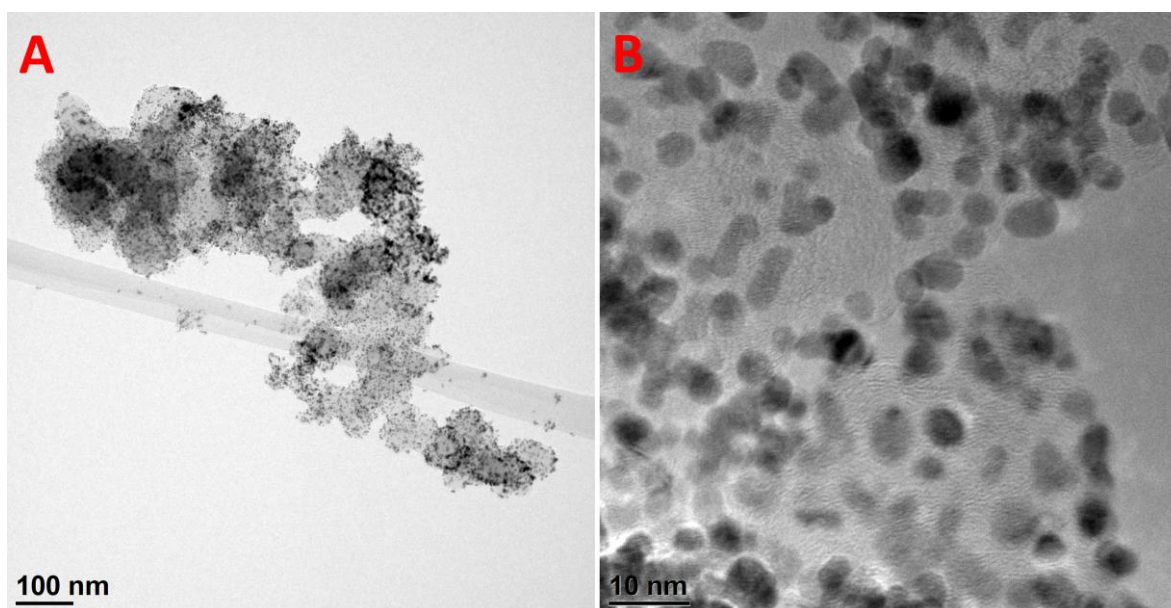


Figure 1. TEM images of Vulcan XC-72R supported catalyst at different magnitude.

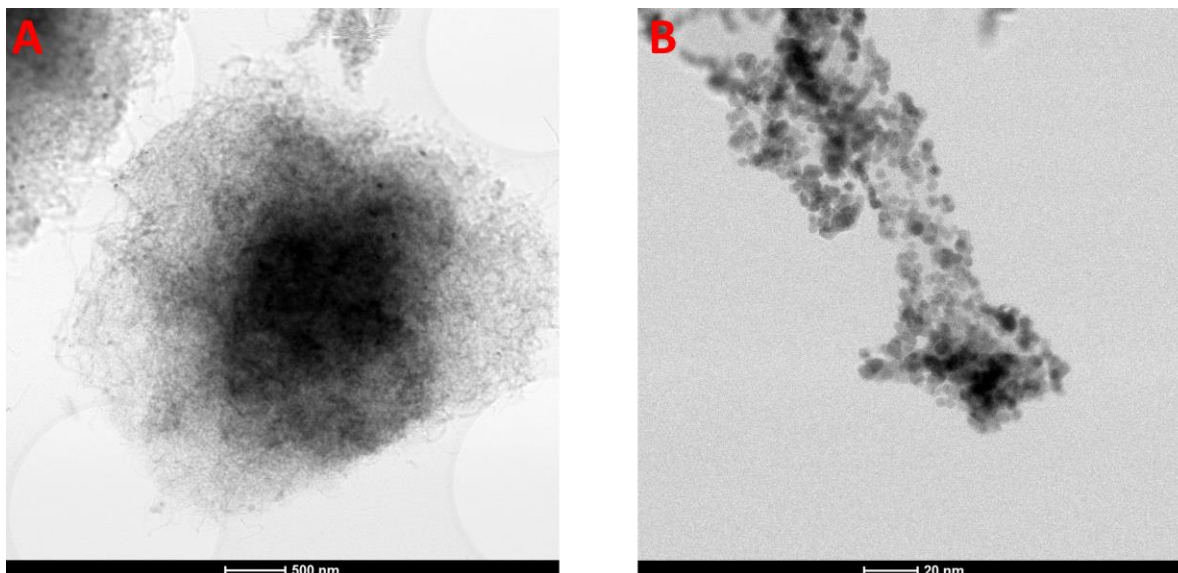


Figure 2. TEM images of carbon nanofibers and carbon nanofibers supported catalyst.

One can see from Fig. 3 that for the system with a limited thickness the “real” percolation (the situation when practically 100% of the particles, their agglomerates and clusters are in a percolating system and a quasi-infinite catalyst cluster appears) starts at about 70% of the catalyst particles volume fraction. This value is significantly higher than the theoretical value for an infinite layer - 33%.

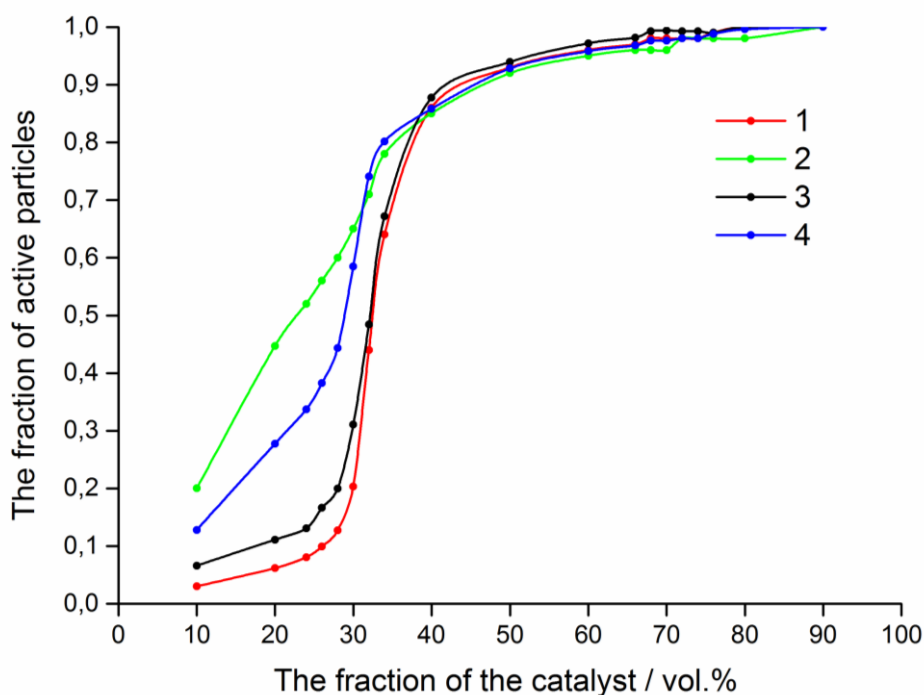


Figure 3. The dependence of the active catalyst particles fraction in the catalyst layer upon the catalyst volume concentration for: (1) – 0.4 μm particles; (2) - 4 μm particles; (3) - a mixture of 0.4 μm particles with 10 vol.% of 4 μm particles; (4) - a mixture of 0.4 μm particles with 20 vol.% of 4 μm particles.

This effect is associated with an influence of the catalyst layer boundaries where continuous chains of catalyst particles and ionomer “particles” are cut off by the membrane or GDL surfaces. So, the concentration of active catalyst particles at the border of the membrane is decreased, because separate catalyst particles and clusters disconnected from the quasi-infinite cluster are appeared. These catalyst particles and clusters do not have an electric contact with the GDL. It is important that for particles with larger sizes the part of active particles increases significantly faster with the catalyst concentration (Fig. 3). In the case of the mixture of particles of the both types a rather strong increase of active particles concentration starts also at lower fraction of the catalyst particles in comparison with the small particles. But it becomes practically important only at significant concentration of large particles - more than 20 vol.% when clusters of such particles (3-5 particles) appear. So, the usage of such mixtures may have some advantages in comparison with the small particles only. The percolation limit also reduces for the particles without regular form (for example for elongated particles [18]) but such an effect is insignificant in our case when the catalyst layer size is comparable with the particles size. The dependence of the active surface area (the contact surface area between the catalyst particles (their chains and agglomerates) and ionomer upon the volume concentration of particles) is shown in Fig. 4.

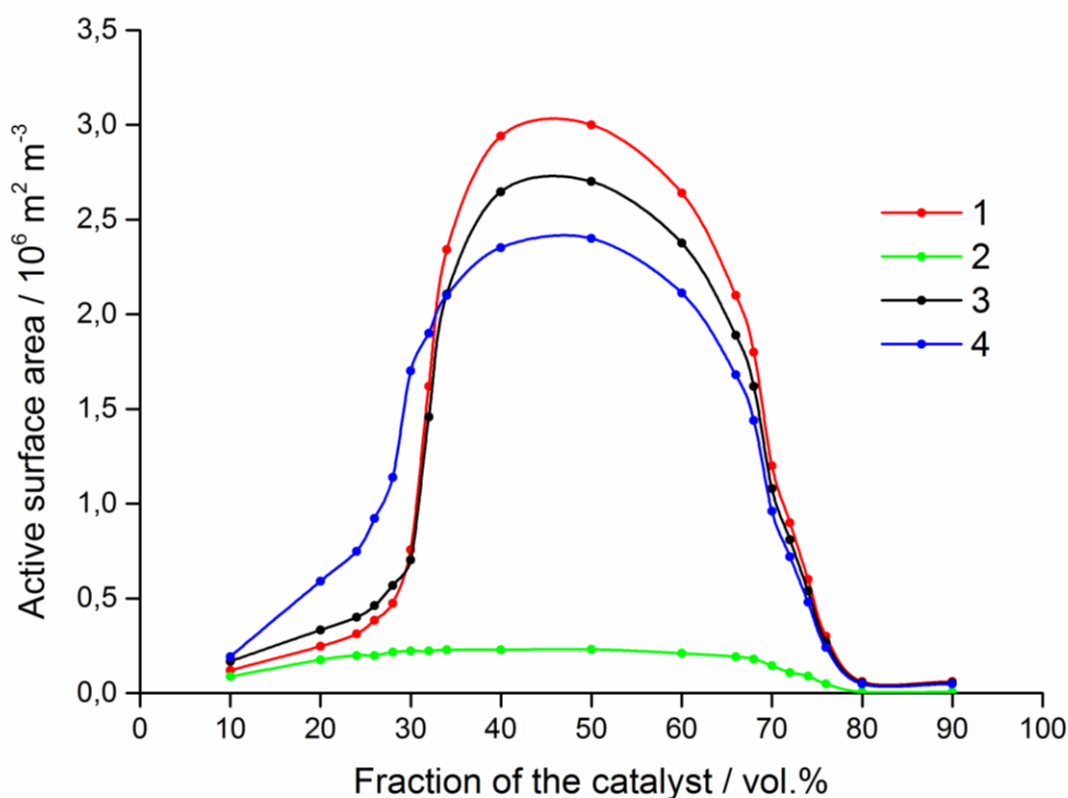


Figure 4. Dependence of the active surface area (a contact surface between the catalyst particle and the ionomer)* in a volume unit upon the catalyst particles volume concentration for: 1 – 0.4 μm particles; 2 - 4 μm particles; 3 – mixture of 0.4 μm particles with 10 vol.% of 4 μm particles; 4 - mixture of 0.4 μm particles with 20 vol.% of 4 μm particles. *The internal particle surface isn't taken into account..

Initially the active surface area increases as the concentration of active particles increases. Maximum active surface area is achieved at 40-50 vol.% of the catalyst particles in the case of small particles and their mixtures with large particles (10-20 vol.%). For large particles maximum active surface area is reached at 35-40 vol.% The further increase of the catalyst particles concentration results in the active surface decreasing due to the decrease of the ionomer concentration and the contact surface between the ionomer and catalyst particles. Certainly, smallest particles have the largest active surface only if an external surface of particles is considered. The large particles in this case have a small contact surface (see Fig.4) and are not able to provide a high catalyst layer efficiency. When the mixture of small particles with the particles of larger size (20 vol.%) is used the maximum active surface area is lower in comparison with the maximum active surface area of small particles, but significant increase of the active surface area begins at a lower particles concentration (at about 20-25 vol.%).

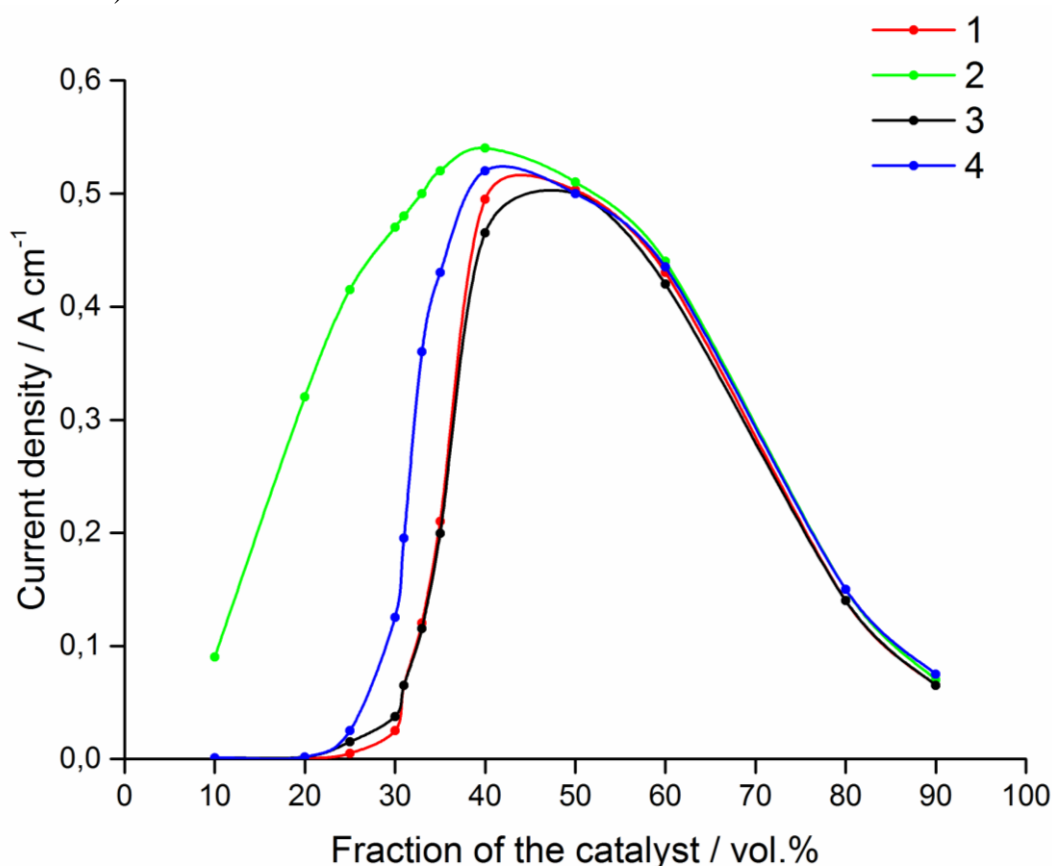


Figure 5. Dependence of current density upon the catalyst volume concentration for: 1 – 0.4 μm particles; 2 - 4 μm particles; 3 – a mixture of 0.4 μm particles with 10 vol.% of 4 μm particles; 4 - a mixture of 0.4 μm particles with 20 vol.% of 4 μm particles. Pt content in the catalyst was assumed - 40% weight, catalyst EASA – 41 $\text{m}^2 \text{g}^{-1}$.

For the mixture with a lower concentration of large particles (10 vol.%) such an effect is negligible because the clusters of large particles almost don't appear and their influence on the percolation threshold is insignificant. The ohmic losses in the catalyst layer and the decrease of potential difference between catalyst particles and ionomer particles are mainly determined by the ionomer. The ionomer can also have a positive effect on reactants/products mass-transfer. So, an

efficient percolation at a lower catalyst particle concentration allows to increase the ionomer concentration together with the appropriate decrease of its resistance and the optimization of the mass-transport. But if Pt particles situated only on the external agglomerates surface can participate in the electrochemical process then the total active surface area in the case of large agglomerates would be too small. It may also result in some decrease of the active surface area for mixed supports. As Pt EASA determined by cyclic voltammetry curves is rather similar for Vulcan XC-72R and nanofibres supported catalysts we supposed that almost all the internal surface of agglomerates is available for electrochemical processes. The numerical evaluation of the fuel cell current density upon the catalyst particle concentration was also made according to such an assumption (see Fig. 5). According to Fig. 5 large agglomerates provide a relatively fast current density increase upon concentration which starts at 10 vol.% of the catalyst concentration in the layer. A maximum current density for the large particles is higher and observed at a little bit lower catalyst particles concentration due to the efficient percolation. In the case of mixed support containing 10 vol.% of the large particles the increase of current density starts practically at the same concentration (30-35 vol.%) as in the case of the small particles. But for the mixture with 20 vol.% of the large particles a significant increase of the current density starts at the catalyst particle concentration of about 26-31 vol.%. Numerical estimations show that at the large particles concentration of about 20 vol.% particles start to associate in clusters containing 3-5 particles (contrary to the situation with large particle concentration of 10 vol.% when clusters almost don't appear). These clusters have a good electric contact with the GDL as their dimensions are comparable with the layer thickness. So, numerical data show that application of particles with the different size can provide a decrease of Pt loading up to 30% at the current density of about 0.5 A cm^{-2} and/or an increase of current density up to 20% at the catalyst particles concentration in the catalyst layer of about 35-40 vol.%.

Some percolation calculations for PEMFC catalyst layers were executed [27-33]. In these calculations models with one size of particles were used and the boundary effects (which are taken into account in this work) were not considered. It was shown that for the achievement of a high generated current an optimum ratio of catalyst/polymer is required. Calculations data [15-17, 32-33] are in a good agreement with experimental data [7, 8, 34, 35], where the optimum concentration of ionomer in the catalyst layer was 20-30 vol.%. An increase of the particle size provides an increase of the electronic conductivity but it reduces the efficiency of the catalyst layer due to diminishing of the catalyst particles active surface (an internal surface of the particles was not taken into account). The consideration of border effects, an internal particle surface and the addition of particles of larger sizes, as it was shown in presented work, predict the shift optimum polymer fraction in the catalyst layers to greater values. As it was examined in refs. [18, 29-31], the water balance and the water transfer in the catalyst layer have a major influence on the layer performance. Water distribution in the catalyst layer is described particularly in [18]. Water is present both in pores and in ionomer particles located in the layer. Therefore the application of the layers with an increased amount of the ionomer without loss of electronic conductivity must result in the optimization of the water balance in the catalyst layer, an increase of ionic conductivity and an increase of the generated current.

The experimental verification of the numerical data was done with the two catalysts and their mixtures with the same Pt concentration. Both catalysts synthesized on nanofibers and Vulcan XC-72R

had rather similar EASA ($41 \text{ m}^2\text{g}^{-1}$ and $45 \text{ m}^2\text{g}^{-1}$, respectively, as mentioned in Section 2.2). A little bit smaller EASA of nanofibers supported catalyst may be attributed to a smaller specific surface area of nanofibers (according to Section 2.2) and low efficiency of Pt atoms penetration inside the agglomerates of nanofibers during magnetron sputtering. It results in an increase of Pt particles size on nanofibers agglomerates. Studies of the fuel cell performance show (Fig. 6) that the difference between the Vulcan XC-72R and the nanofibers supported catalysts is not significant though the nanofibers supported one has a little bit lower activity. According to the results we supposed that the most part of Pt particles which are inside of large nanofibers agglomerates can participate in the electrochemical process at relatively low current density. So, water, reactant gases and the ionomer (partially) can penetrate inside agglomerates. Certainly, along with the increase of the current density some mass-transport limitations can take place inside the agglomerates. It was also taken into account for numerical estimation of the current density which could be generated by different type of agglomerates with Pt catalyst (Fig. 5). The experimental dependence of the current density upon the catalyst volume concentration (Fig. 6) was of the same type for Pt on both carbon supports and their mixtures.

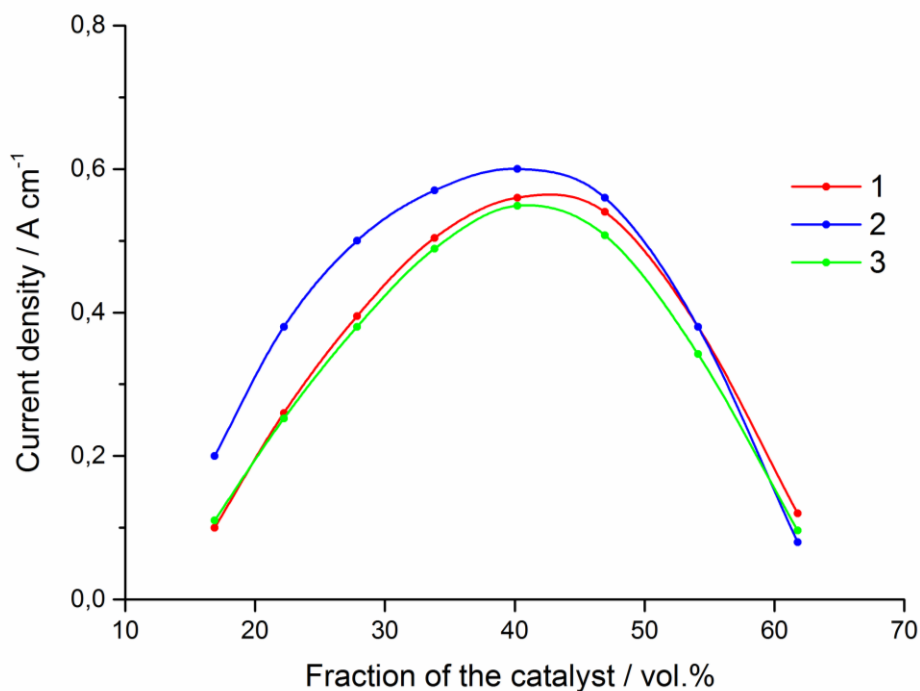


Figure 6. Experimental data of the PEMFC current density dependence upon the catalyst volume concentration on oxygen electrode for Pt based catalyst on different supports: 1 - Vulcan XC-72R; 2 - Vulcan XC-72R with 20 vol.% of nanofibers; 3 - nanofibers. PEMFC voltage – 0.7 V; catalyst loading is 1.75 mg cm^{-2} ; hydrogen pressure is 1 bar; air flow - 2 L min^{-1} .

The results in Fig. 6 are in an appropriate qualitative agreement with the numerical data (Fig. 5). For both carbon supports and their mixtures the maximum current density was observed at the catalyst concentration of about 40-45 vol.% which correlates with the theoretical data. In the case of smaller particles (agglomerates) the highest current density was at a little bit higher catalyst concentration due to a worse agglomerates contact with each other and with the GDL (lower

percolation). Also in case of the mixture of supports the current density reaches a higher value already at the catalyst concentration in the layer of about 37-40 vol.%. More detailed data of the current density dependence upon the catalyst support composition (see Table 1) show that the best results are obtained for mixture with nanofibers concentration of about 20-30 vol.%.

Table 1. Dependence of current density upon the catalyst support composition at the catalyst concentration of about 40 vol.% (PEMFC voltage of 0.7 V; catalyst loading is 1.75 mg cm^{-2} ; reactant (hydrogen and air) pressure is 1 bar; air flow - 2 L min^{-1}).

Catalyst type	Current density, A cm^{-2} at 0.7 V
Vulcan XC-72R	0.561
Vulcan XC-72R with 10 vol.% of nanofibers	0.565
Vulcan XC-72R with 20 vol.% of nanofibers	0.605
Vulcan XC-72R with 30 vol.% of nanofibers	0.601
Vulcan XC-72R with 50 vol.% of nanofibers	0.560
Carbon nanofibers	0.548

Fig.6 and Table 1 also demonstrate that at the catalyst concentration of about 40 vol.% in the catalyst layer the use of the mixture of catalyst carriers (Vulcan XC-72R with 20 vol.% nanofibers) provides about 10% higher fuel cell efficiency (higher current density) in comparison with pure Vulcan XC-72R supported Pt catalyst. The decrease of the current density with the further increase of nanofibers concentration may be attributed to the decrease of the total Pt catalyst surface in the mixed catalyst and some transport limitations inside nanofibers agglomerates. In our recent studies [34-35] we showed that the addition of reduced graphene oxide to the active layers of the fuel cell in the amount of about 1-5 wt.% significantly improves its performance. These results are in a rather good agreement with the presented results of numerical estimations (large size of graphene flakes and their agglomerates).

The effect of PEMFC performance increase using new nanomaterials such as nanotubes, nanofibers, carbon aerosols was experimentally observed earlier [1-4]. In these articles, the authors suggest that the improvements in performance of the catalyst layers relates only to the increase of catalytic activity of Pt particles on these types of carbon supports.

In present study the other effects are considered, which are related to percolation and catalyst layer structure. Namely it is a positive influence of the addition of nanofibers supported catalyst with a large agglomerates size to a traditional carbon black supported catalyst on the catalyst layer activity. The catalytically active internal surface of agglomerates was taken into account. Such additives result in a better electric contact of catalyst particles and, accordingly, permit to increase the ionomer concentration. The increase of ionomer concentration, in its turn, reduces the resistance of the catalyst layer for ionic current, improves mass transport and stabilizes water balance in the layer. The results of pilot tests are in a good agreement with theoretical calculations.

4. CONCLUSIONS

The PEMFC catalyst layer structure and electrochemical parameters were analyzed using a numerical model with a random catalyst particles (particle agglomerates) distribution in a polymer (ionomer) porous matrix. An electrochemical activity of the internal surface of agglomerates was taken into account in the calculations. Application of such Monte Carlo simulation method to the catalyst layer with particles of two different sizes predicted a possibility of the ionomer concentration increase and a decrease of the ohmic losses associated with ion transport in the catalyst layer together with an improvement of water balance and mass transport. The main attention was paid to the Pt-based catalyst supported on the Vulcan XC-72R and carbon nanofibres agglomerates. It was shown that the formation of the catalyst particle clusters (particle agglomerates) for small particles (Vulcan XC-72R) starts at the catalyst concentration in the layer of about 30 vol.%. With the further catalyst concentration increase the amount of active particles achieves maximum at about 60 vol.%, when practically all the catalyst particles are becoming a part of a quasi-infinite cluster with electronic conductivity. For large particles (nanofibres) the generation of active clusters starts at lower catalyst concentration (about 10 vol.%) and it permits to involve a larger amount of catalyst in the electrochemical process at a lower catalyst concentration. Mixtures of such particles also have a lower threshold for beginning of percolation which becomes significant already at 20 vol.% of large particles in the catalyst mixture. This effect is caused by the beginning of the formation of clusters containing 3-5 large particles which size is comparable to the catalyst layer thickness. In all cases the dependence of the catalyst active surface area and the current density upon the catalyst concentration have a maximum which appears at a lower catalyst volume concentration in the layer for larger particles and their mixture with smaller particles. The numerical estimations demonstrated a possibility of precious metal loading reduction up to 30% and/or fuel cell performance increasing (current density) up to 20% just due to the addition of nanofibers (large particles) to the catalyst composition. The fuel cell tests demonstrated that the dependence of the current density upon the catalyst concentration has a distinct maximum which appears at a lower catalyst concentration for nanofibers (large particles) and their mixtures. The combined application of the Vulcan XC-72R supported catalyst together with the nanofibers supported catalyst (about 20-30 vol.% of the catalyst composition) permitted to increase PEMFC current density for about 10%.

ACKNOWLEDGEMENTS

This work was done at the partial financial support of the Russian Scientific Foundation (project number 14-29-00111)

References

1. K. Lee, J. Zhang, H. Wang and D.P. Wilkinson, *J. Appl. Electrochem.*, 36 (2006) 507.
2. A. Kongkanand, S. Kuwabata, G. Girishkumar and P. Kamat, *Langmuir*, 22 (2006) 2392.
3. E. Antolini, *App. Catal. B. Environ.*, 88 (2009) 1.
4. C. Moreno-Castilla, F.J. Maldonado-Hodar, *Carbon*, 43 (2005), 455.
5. C.C. Sung, C.Y. Liu, C.C.J. Cheng, *Int. J. Hydrogen Energy*, 39 (2014) 11712.

6. S. Park, Y. Shao, H. Haiying, P.C. Rieke, V.V. Viswanathan, S.A. Towne, *Electrochem. Commun.*, 13 (2011) 263.
7. E. Passalacqua, F. Lufrano, G. Squadrito, A. Patti, L. Giorgi, *Electrochim. Acta*, 46 (2001) 799.
8. E. Antolini, L. Giorgi, A. Pozio, E. Passalacqua, *J. Power Sources*, 77 (1996) 297.
9. Y. Bultel, P. Ozil, R. Durand, *J. Appl. Electrochem.*, 30 (2000) 1369.
10. Y. Bultel, P. Ozil, R. Durand, D. Simonsson, *Electrochem. Soc. Proceedings*, 95 (1995), 34.
11. Y.W. Rho, S. Srinivasan, Y.T. Kho, *J. Electrochem. Soc.*, 141 (1994) 2089.
12. D. Harvey, J.D. Pharoah, K. Karan, *J. Power Sources*, 179 (2008) 209.
13. W.K. Epting, S. Litster, *Int. J. Hydrogen Energy*, 37 (2012) 8505.
14. R.M. Rao, R. Rengaswamy, *Chem. Eng. Res. Des.*, 84 (2006) 952.
15. V.N. Fateev, I.E. Baranov, A.V. Sysoev, *Russ. J. Electrochem.*, 33 (1997) 893.
16. V.N. Fateev, A.A. Fridman, O.I. Archakov, I.E. Baranov, A.V. Davletchin, I.A. Kirillov, *Russ. J. Electrochem.*, 30 (1994) 1377.
17. I.E. Baranov, V.N. Fateev, A.V. Sysoev, M. Tsyppin, Mathematical model of PEM-Fuel Cell catalytic layer, Proceedings of the Hypothesis II Symposium, Grimstad, Norway, 1997, 597.
18. I.E. Baranov, S.A. Grigoriev, D. Ylitalo, V.N. Fateev, I.I. Nikolaev, *Int. J. Hydrogen Energy*, 31 (2006) 203.
19. V.N. Fateev, I.E. Baranov, A.V. Sysoev, V.D. Rusanov, *Doklady Chemical Technology*, 354 (1997) 55.
20. I.E. Baranov, V.N. Fateev, *RF Patent*, RU 2 015 619 590, 2015.
21. Yu. G. Chirkov, V. I. Rostokin, *Russ. J. Electrochem.*, 40 (2004) 27.
22. A.A. Fedotov, S.A. Grigoriev, E.K. Lyutikova, P. Millet, V.N. Fateev, *Int. J. Hydrogen Energy*, 38 (2013) 426.
23. S.A. Grigoriev, A.A. Fedotov, S.A. Martemianov, V.N. Fateev, *Russ. J. Electrochem.*, 50 (2014) 638.
24. O.K. Alexeeva, V.N. Fateev, *Int. J. Hydrogen Energy*, 41 (2016) 3373.
25. S.A. Grigoriev, P. Millet, V.N. Fateev, *J. Power Sources*, 177 (2008) 281.
26. S.A. Grigoriev, E.K. Lyutikova, S. Martemianov, V.N. Fateev, *Int. J. Hydrogen Energy*, 32 (2007) 4438.
27. B. I Shklovskii, A. L Efros, Berlin, Springer Series in Solid-State Sciences, 45 (1984).
28. Yu. Chirkov, V. Rostokin, *Alternative Energy and Ecology (ISJAEE)*, 192 (2016) 43
29. Yu. Chirkov, V. Rostokin, *Alternative Energy and Ecology (ISJAEE)*, 189 (2016) 76.
30. Yu. Chirkov, V. Rostokin, *Alternative Energy and Ecology (ISJAEE)*, 190 (2016) 105.
31. Yu. Chirkov, V. Rostokin, A. Kuzov, *Russ. J. Electrochem.*, 52 (2016) 123.
32. Yu. Chirkov, V. Rostokin, *Russ. J. Electrochem.*, 50 (2014) 872.
33. Yu. Chirkov, V. Rostokin, *Russ. J. Electrochem.*, 50 (2014) 235.
34. A.S. Pushkarev, I.V. Pushkareva, S.A. Grigoriev, V.N. Kalinichenko, M.Yu. Presniakov, V.N. Fateev, *Int. J. Hydrogen Energy*, 40 (2015) 14492.
35. S.A. Grigor'ev, A.S. Pushkarev, V.N. Kalinichenko, I.V. Pushkareva, M.Yu. Presnyakov, and V.N. Fateev, *Kinet. and Catal.*, 56 (2015) 689.